Preparation and Characterization of the Magnetic Fluid of Trimethoxyhexadecylsilane-Coated Fe_3O_4 Nanoparticles

Hyun Gil Cha,[†] Chang Woo Kim,[†] Shin Woo Kang,[‡] Byung Kyu Kim,[§] and Young Soo Kang*,[†]

Department of Chemistry, Sogang University, Shinsu-dong #1, Mapo-gu, Seoul 121-742, Republic of Korea, Central Coporation R&D Center, 54 Seongsan-Dong, Changwon City, Kyungnam 641-315, Republic of Korea, and Department of Polymer Science and Engineering, Pusan National University, Busan 609-735, Korea

Received: December 25, 2009; Revised Manuscript Received: April 28, 2010

A new magnetic fluid was prepared by colloidal dispersion of paramagnetic Fe_3O_4 nanoparticles coated with monomolecular adsorbed monolayer films of long-chain trimethoxyhexadecylsilane (THS) in a nonpolar hydrocarbon oil. The magnetic Fe_3O_4 nanoparticles were characterized by using TEM, XRD, FT-IR, and VSM. The silanization of the magnetic particle surface was conducted in methanol. The silanized films on the magnetic particles are characterized with FT-IR spectroscopy. The optical absorbance of the magnetic particle versus concentration of the solution was measured with a UV−vis spectrophotometer and shows a linear increase of absorbance. Langmuir behavior of the THS-coated Fe_3O_4 nanoparticles at the air/water interface was characterized with pressure−area isotherms and Brewster Angle Microscopy. The collapse pressure of the Langmuir monomolecular films was determined as 62 mN/m. The stability of magnetic fluids of the THS-coated Fe_3O_4 nanoparticles are comparatively studied with the conventional oleic acid-coated magnetic fluid of Fe_3O_4 nanoparticle at the acidic condition of pH 4. The durability of the magnetic fluid of THS-coated Fe_3O_4 nanoparticles is shown as it lasted longer than 60 days.

Introduction

The magnetic fluid, often called as a ferrofluid, is a kind of suspension of magnetic particles such as magnetite (Fe_3O_4), iron (Fe), nickel (Ni), and cobalt (Co) of the size of colloids dispersed into the carrier liquid. Even if centrifugal force or magnetic field continues to work, the ferromagnetic particles and liquid are not separated and the fluid behaves as if it was a magnetism itself.[1,2] Due to the small size and superparamagnetic behavior, these magnetic nanoparticles exhibit different physical properties from their bulk counterparts. Magnetic fluids have been used commercially for a number of years in numerous devices, such as rotating shaft seals and exclusion seals, loud speakers, dampers, etc., by using their unique superparamagnetic, tribological, thermal, and mechanical properties.[3−5] Recently, investigation of novel uses of magnetic particles in the separation area has increased significantly. Magnetic particles with appropriately modified surface characteristics can be used to make an easy separation of biomolecules, to sort specific cell types from a cell population, or to deliver drugs to a target organ in the body.[6] Thus, the separation of magnetic fluids has continued to attract a great deal of attention since their inception in the late 1960s. A difficulty associated with the preparation of magnetic fluids is that the particles have large surface area-to-volume ratios and thus tend to aggregate to reduce their surface energy. In addition, magnetic dipole−dipole attraction between particles enhances the difficulties experienced in the preparation of magnetic fluids in comparison to nonmagnetic nanoparticles. Prevention of magnetic nanoparticle agglomeration is one of the critical obstacles to be overcome in producing stable magnetic fluids. To prevent aggregation of magnetic nanoparticles, the particle surfaces have to be coated with organic surfactants. As a result, the magnetic fluids are a stable colloidal system consisting of rather small (3−10 nm in size) surfactant-coated ferromagnetic particles dispersed in a liquid carrier. Generally, magnetic fluids have been prepared by coating the magnetic particle surface with a fatty acid such as oleic acid.[7,8] The coated particles are dispersed into an oil such as kerosene. Although this method is a simple and easy preparation, it has a problem since the oleic-type surfactant only adheres to the surface of the fine ferromagnetic particles through electrostatic attraction. So the surfactant would dissociate from the particle surfaces if they are affected by an external effect such as a polar solvent or the effect of thermal and applied external current, causing agglomeration of the particles. Thus, the magnetic fluid prepared by the conventional method was not keeping a stable dispersion after long-term use.[9] In this study, we have studied the preparation and characterization of ferromagnetic fluids consisting of Fe_3O_4 magnetic particles. The Fe_3O_4 nanoparticles were coated with trimethoxyhexadecylsilane (THS) to solve such problems of the conventional magnetic fluid. This resulted in stable magnetic fluids with a high magnetization value for longer duration.

Experimental Sections

Materials. Iron(II) chloride tetrahydrate (SHINYO Pure Chemicals Co.), iron(III) chloride hexahydrate (ACROS Organics Co.), sodium hydroxide and HCl (JUNSEI Chemical Co.), glacial acetic acid (KATAYAMA Chemical Co.), glycerol (SHINYO Chemical Co.), methanol (Haxman Limited), and trimethoxyhexadecylsilane (THS) (Fluka) were obtained from commercial sources. All chemicals were generally reagent grade and were used as received.

Synthesis of Trimethoxyhexadecylsilane-Coated Fe_3O_4 Magnetic Fluid. Magnetite (Fe_3O_4) nanoparticles used in this study were prepared according to the precipitation technique

* To whom correspondence should be addressed. E-mail: yskang@sogang.ac.kr.
[†] Sogang University.
[‡] Central Coporation R&D Center.
[§] Pusan National University.

10.1021/jp912166b
Published on Web 05/11/2010

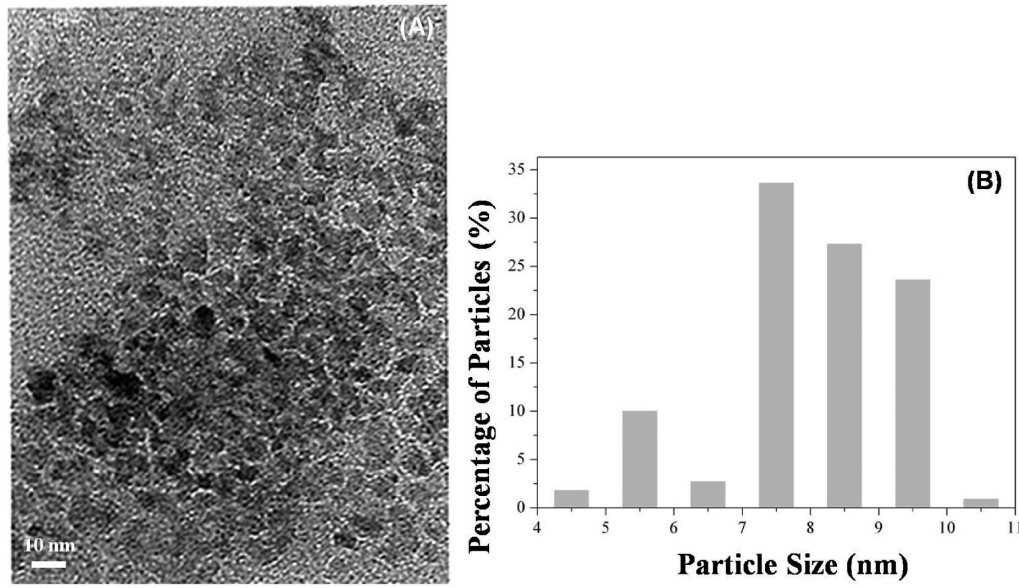

Figure 1. Transmission electron microscopic image (A) and particle size distribution of synthesized Fe_3O_4 nanoparticles (B).

described by Shimoiizaka and Reimer.[7] Fe_3O_4 nanoparticles were prepared at pH 11−12 by precipitation of divalent (Fe^{2+}) and trivalent (Fe^{3+}) iron salts in an alkaline medium (sodium hydroxide) with mechanical stirring, after adjusting the mole ratio of Fe^{2+}/Fe^{3+} to 0.5 by using $FeCl_2 \cdot 4H_2O$ (43 g) and $FeCl_3 \cdot 6H_2O$ (116.8 g) solutions. The precipitated magnetite particles (50 g) were neutralized with 2.0 N HCl and then washed five times with distilled water to remove the formed electrolyte. The water was then replaced with methanol and the washing was repeated five times by aspiration. Hereafter, the prepared magnetite particles were placed into a 2.0 L three-necked flask containing 1.5 L of methanol and adjusted pH to 4.5 with glacial acetic acid. After THS (55.3 mL) was added to the flask, the suspension was heated to 65 °C for 2 h under nitrogen bubbling and mechanical stirring. In this work, the amount of added silane was 1.5 times that of the minimum covering amount of the surface area of magnetite particles.

The silanized magnetite slurry was then transferred into a 2.0 L glass beaker containing 300 mL of glycerol and heated on a hot plate until a temperature of 160−170 °C was reached. The mixture was allowed to cool to room temperature. Both the heating and cooling steps were performed with stirring under nitrogen. The glycerol particle slurry was transferred into 1.0 L of water in a 2.0 L of beaker, then the particles were washed five times with water. After filtering, the particles were dried in a vacuum oven at 80 °C for 12 h. The magnetic fluid was prepared by changing the content of particles from 10 to 70 g in 100 mL of kerosene.

Characterization. The size and morphology of the particles were determined with TEM (JEOL 200 CX) images. The samples were prepared by evaporating dilute suspensions on a carbon-coated film. The powder X-ray diffraction allowed the identification of the crystalline structure of particles, using an automated diffractometer Philips X'Pert-MPD system with Cu Kα radiation source (λ = 1.54056 Å). Magnetization was measured at room temperature in a vibration sample magnetometer (LakeShore, VSM7300) up to a field of ±15 kOe. The infrared spectra of dried samples inserted into the KBr powder were recorded on a FT-IR (Perkin-Elmer Spectrum 2000) computerized absorption spectrophotometer in the wavelength range 4000−170 cm^{-1}. Optical absorbance of magnetic fluid was measured with a Hitachi model U-3210 spectrophotometer.

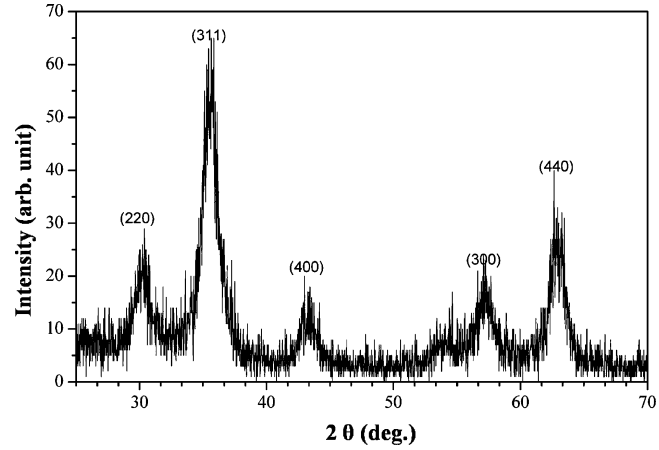

Figure 2. X-ray diffraction of the synthesized Fe_3O_4 nanoparticles.

The contact angle of the silanized Fe_3O_4 nanoparticles was determined with a contact angle meter (Kruss, Contact Angle Measuring System G2). The Langmuir behavior of the monolayer of silanized Fe_3O_4 nanoparticles at the air/water interface was studied with a pressure−area isotherm, using a Langmuir trough (KSV Minitrough and KSV 2000 System) and a Brewster Angle Microscopy (BAM, Nanofilm Tech.). The stability of the magnetite fluid was studied by measuring the setting height of particles from the upper layer of the magnetic fluid that is contained in the test tube (height is 120 nm) at pH 4. The average surface area of synthesized Fe_3O_4 nanoparticles was determined by using the BET (Quantachrome Autosorb-1VP/Kr/MP) method with nitrogen as the carrier gas.

Results and Discussion

Characterization of Synthesized Magnetite (Fe_3O_4) Particles. Panels A and B of Figure 1 show the TEM image and particle size distribution of synthesized Fe_3O_4 nanoparticles. As shown in the figure, the synthesized magnetite particles have an irregular spherical shape. The average particle size was determined by TEM images to be 7.5 nm and an average surface area based in the BET method with nitrogen adsorption as the carrier gas was determined as 148.4 m^2/g. The XRD pattern of prepared magnetite particles is given in Figure 2. Obviously

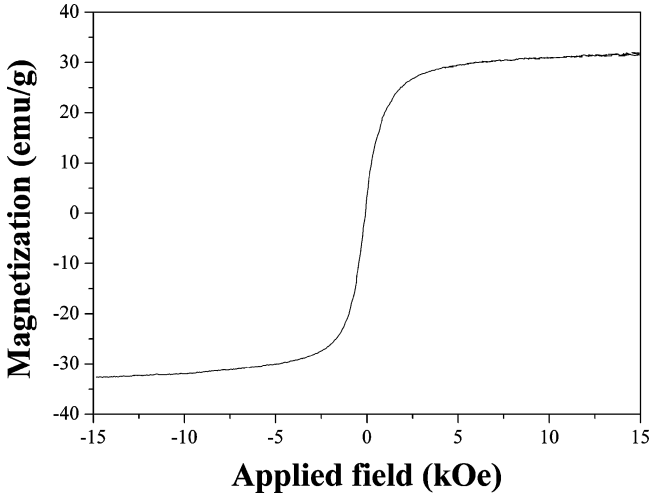

Figure 3. Magnetization curve as a function of applied field of synthesized Fe_3O_4 nanoparticles with 7.5 nm of mean diameter at room temperature.

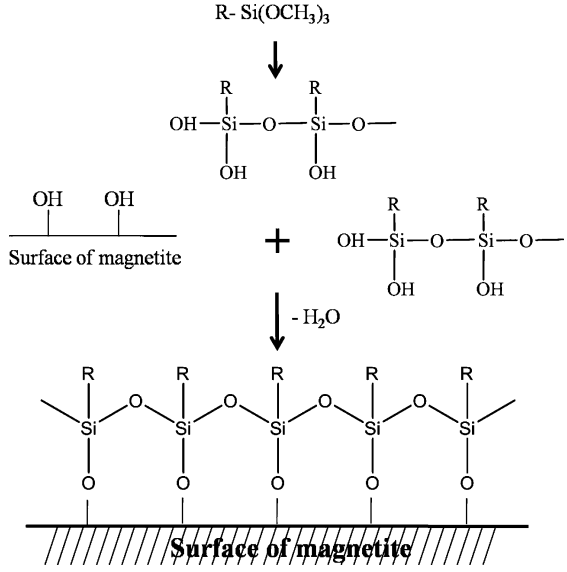

Figure 4. Schematic illustration of the process for silanization of synthesized Fe_3O_4 nanoparticle surface with THS.

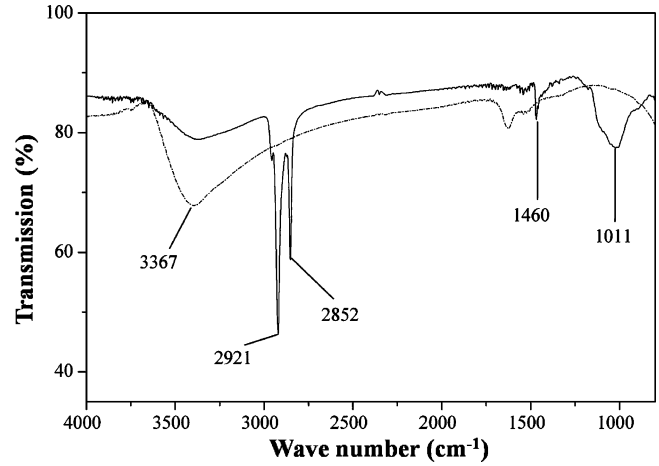

Figure 5. FT-IR spectra of naked Fe_3O_4 nanoparticles (---) and THS-coated Fe_3O_4 nanoparticles (—).

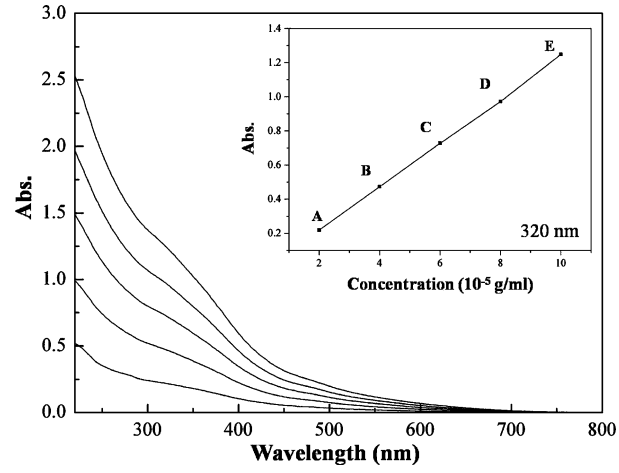

Figure 6. UV−vis absorption spectra of THS-coated Fe_3O_4 nanoparticle suspension in $CHCl_3$ and optical absorption data of THS-coated Fe_3O_4 nanoparticle suspension at $\lambda_{max} = 320$ nm versus concentration of THS-coated Fe_3O_4 nanoparticles solution: (A) 2×10^{-5} g/mL; (B) 4×10^{-5} g/mL; (C) 6×10^{-5} g/mL; (D) 8×10^{-5} g/mL; and (E) 10×10^{-5} g/mL).

the peaks are very broad due to the small particle size. The average particle size of the sample was determined as 6.8 nm by using Scherer's equation from the half-maximum width of the (311) X-ray diffraction line.[12] The different particle size was assumed as a result of slight oxidation of the surface of magnetite particles during experimental procedure.

Bulk Fe_3O_4 is ferromagnetic at room temperature, but below a critical particle size it becomes superparamagnetic and shows small coercivity.[13] When a field is applied at bulk ferromagnetic materials, there is a tendency for each magnetic moment to turn toward the direction of the magnetic field. If no opposing force acts, complete alignment of the magnetic moment would be produced and the specimen as a whole would acquire a very large moment in the direction of the field. But when the specimen diameter is below the transition of polydomain to single domain size (in the case of Fe_3O_4, the size is 34 ± 5 nm), the thermal agitation by rotation of the particle in the course of magnetization opposes the magnetic alignment and tends to keep the magnetic moment pointed in a random direction. The result is only partial alignment in the field direction, and therefore the susceptibility decreases. Figure 3 shows the magnetization curve of the synthesized Fe_3O_4 nanoparticles at room temperature. The magnetization is 32.2 emu/g at a magnetic field of 15 kOe. The variation of magnetization with an applied field, H (kOe), shows no hysteresis: that is, both the remanence and coercivity are zero. This indicates a superparamagnetic behavior, as expected for the nanoscale dimension of the particles.

Silanization of Magnetic Particles. Figure 4 shows the schematic procedure of the silanization of Fe_3O_4 nanoparticle surface coated with THS.[15] The silanization reaction results in a single layer of monomolecular film of THS on the surface of magnetic particles. The silanization of the Fe_3O_4 nanoparticle surface with THS was identified with FT-IR spectrum and water contact angle measurement. Figure 5 shows the FT-IR spectra of naked Fe_3O_4 nanoparticle (---) and Fe_3O_4 nanoparticle surface coated with THS (—). Naked Fe_3O_4 nanoparticle shows the broad absorption peaks around 3367 cm^{-1} due to the OH group of the particle surface. FT-IR spectra of Fe_3O_4 nanoparticle coated with THS show absorption peaks around 2852 and 1460 cm^{-1}. These peaks are assigned to the alkyl chain of THS. The peaks at 2921 and 1011 cm^{-1} are assigned to the carbon dioxide flow gas and the Si−O bond on the Fe_3O_4 nanoparticle surface, respectively. From these results, we confirmed the chemical

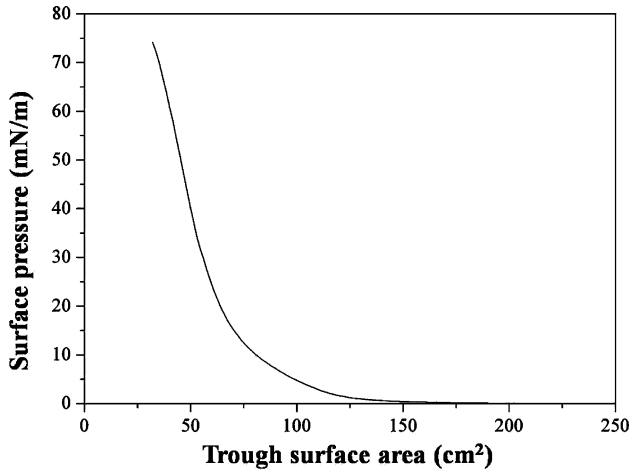

Figure 7. Surface pressure area isotherm of the monolayer of THS-coated Fe_3O_4 nanoparticle at the air/water interface. The aliquot of the 45 μL stock solution was spread on the water surface, of which solution was prepared by dissolving 1 mg of THS-coated Fe_3O_4 nanoparticle in 1 mL of $CHCl_3$ solution.

bonding of THS on the Fe_3O_4 nanoparticle surface. The water contact angle was determined as 78°. This indicates that the Fe_3O_4 nanoparticle surface was coated with THS in a monomolecular film.

Characterization of Magnetic Fluid. Figure 6 shows the UV−vis absorption spectra of the THS-coated Fe_3O_4 nanoparticle magnetic fluid suspension in $CHCl_3$. The optical absorbance data at $\lambda_{max} = 320$ nm versus the concentration of THS-coated Fe_3O_4 nanoparticle in $CHCl_3$ was shown in the inset of the figure. The linear increase of optical absorbance versus concentration of THS-coated Fe_3O_4 nanoparticle in $CHCl_3$ indicates that the Fe_3O_4 nanoparticles are uniformly dispersed in the solution by chemical bonding of THS on the surface of the Fe_3O_4 nanoparticle.

Langmuir Behavior of the THS-Coated Fe_3O_4 Nanoparticle Complex at the Air/Water Interface. Figures 7 and 8 show the surface pressure−area isotherms and Brewster Angle Microscopy images of a monolayer of the THS-coated Fe_3O_4 nanoparticle at the air/water interface, respectively. The monolayer of the THS-coated Fe_3O_4 nanoparticle shows the stable homogeneous monolayer behavior from gas phase to liquid phase, then furthermore to solid phase until a surface pressure of 62 mN/m at which point it collapses. The monolayer shows the zero pressure molecular area (A_o) of one composite particle complex as 88 Å^2. The stable monolayer formation of the composite particles at the air/water interface indicates the homogeneous dispersion of the composite particles in the solution and no aggregation of the Fe_3O_4 nanoparticles. Brewster Angle Microscopy images show that the monolayer of the THS-coated Fe_3O_4 nanoparticle at the air/water interface shows the monomolecular films of the THS-coated Fe_3O_4 nanoparticle were well-formed and stable until a surface pressure of 55 mN/m without any aggregation of the particles. Thereafter it starts to collapse and results in the aggregated one, as indictaed by a white spot in the BAM images, Figure 8C and D.

Figures 9 and 10 show the viscosity and density of the magnetic fluid consisting of THS-coated Fe_3O_4 nanoparticles in kerosene versus the concentration of THS-coated Fe_3O_4 nanoparticles by dissolving it from 10 to 70 g in 100 mL of kerosene as carrier liquid. The presence of colloidal particles in a fluid increases internal friction when it is flowing. This results in an increased viscosity. The viscosity and density of the magnetic fluid are increased with increasing the concentration of THS-coated Fe_3O_4 nanoparticles in kerosene. Those data

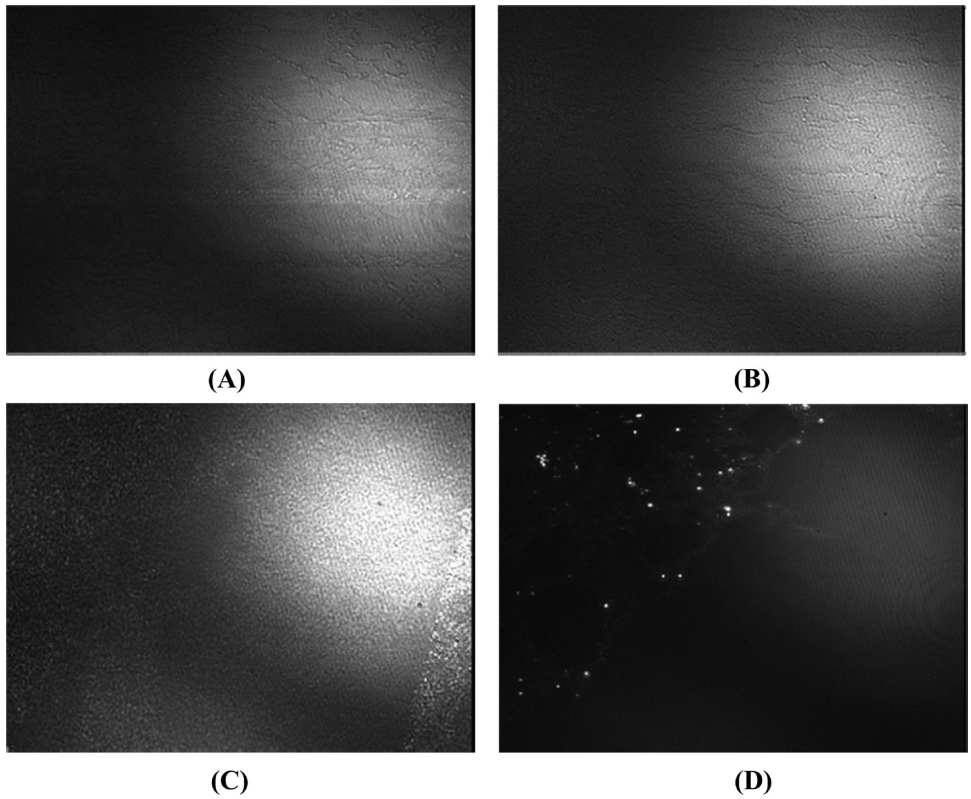

Figure 8. Brewster angle microscopic images of the Langmuir layer of THS-coated Fe_3O_4 nanoparticle on the subphase of pure water at 6 (A), 35 (b), 55 (c), and 62 mN/m (D). The Langmuir monolayer was prepared by spreading 200 μL of stock solution of 1 mg of THS-coated Fe_3O_4 nanoparticle dissolved in 1 mL of $CHCl_3$.

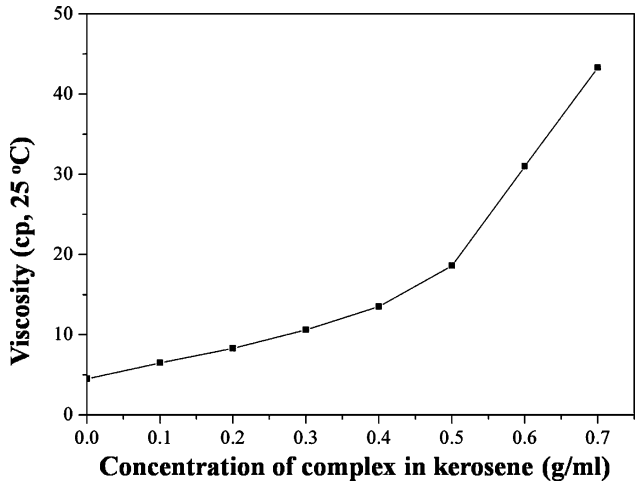

Figure 9. Viscosity of the magnetic fluid consisting of THS-coated Fe_3O_4 nanoparticles in kerosene versus concentration of THS-coated Fe_3O_4 nanoparticles in kerosene.

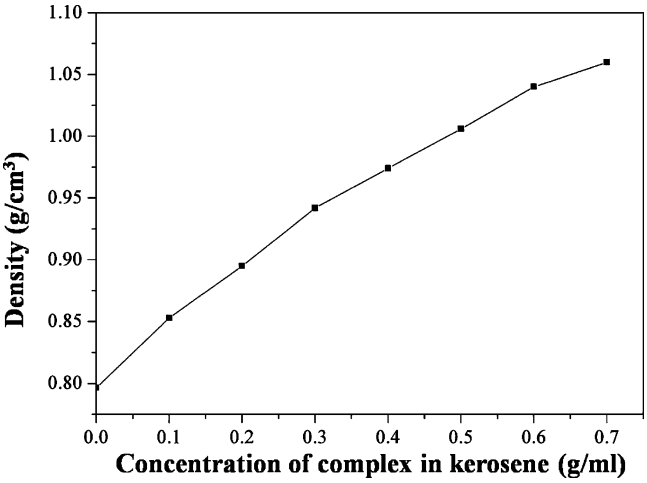

Figure 10. Density of the magnetic fluid of THS-coated Fe_3O_4 nanoparticles in kerosene versus the concentration of THS-coated Fe_3O_4 nanoparticles in kerosene.

are shown in Figures 9 and 10; the viscosity and density of the magnetic fluid with 0.7 g/mL of THS-coated Fe_3O_4 nanoparticles in kerosene are 43.3 cP (25 °C) and 1.06 g/cm^3, respectively.

Figure 11 shows the initial magnetization curve of magnetic fluid with various densities. As can be seen from this figure, magnetic fluids exhibit superparamagnetic behavior characteristics in that they exhibit no remanence and that their magnetization increases with increasing magnetic field, tending toward a saturation value. If there is no interaction between the particles, the magnetization of the synthesized paramagnetic particles in the magnetic fluid can be represented as follows:[7]

$$\sigma = \frac{\sigma_s(\rho - \rho_1)}{\rho(\rho_2 - \rho_1)}\rho_2$$

where σ is the magnetization of the magnetic fluid, σ_s is the magnetization of magnetic particles, ρ is the density of the magnetic fluid, ρ_1 is the density of the liquid carrier, and ρ_2 is the density of magnetic particles. Figure 12 shows the relationship between magnetization and density of the magnetic fluid. The line in Figure 12 is the value calculated with above equation. We used the experimental value of 32.3 emu/g at 15 kOe field for magnetization of magnetic particles. As shown in Figures

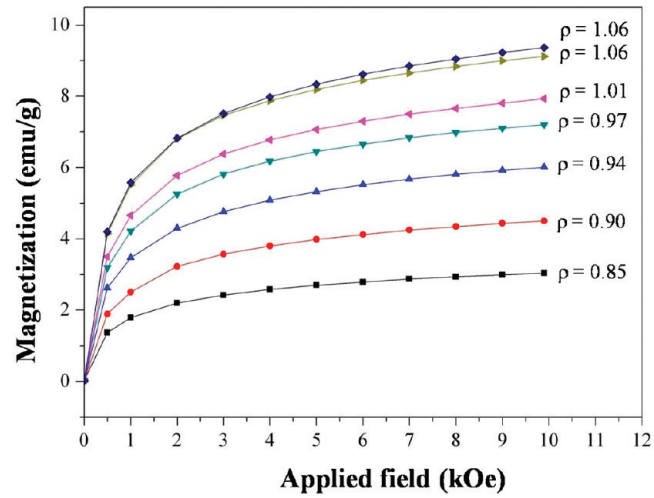

Figure 11. Initial magnetization curves of THS-coated Fe_3O_4 nanoparticles in kerosene with different densities versus applied magnetic field.

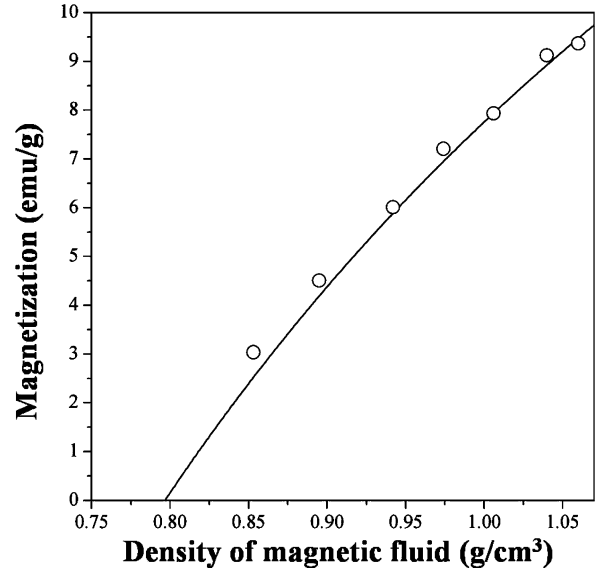

Figure 12. Magnetization data of the magnetic fluid of THS-coated Fe_3O_4 nanoparticles in kerosene versus the density of magnetic fluid.

11 and 12, the measured magnetization is in good agreement with the calculated magnetization of the magnetic fluid. So, it could be acquired for the values of magnetization of synthesized magnetic fluid, if we know the magnetization of the magnetic particles used and the density of the magnetic fluid. Figure 13 shows the dispersion stability of the kerosene base magnetic fluid consisting of THS-coated Fe_3O_4 nanoparticles with duration time. In this figure, the index of stability (I) is as follows:[16−20]

$$I = (\rho_1 - \rho_w)/(\rho - \rho_w)$$

where ρ_l is the density of the upper layer of the magnetic fluid after duration, ρ is the density of the freshly prepared magnetic fluid, and ρ_w is the density of the liquid carrier. As shown in the figure, the THS-coated Fe_3O_4 magnetic fluids do not show any changed value of the index of stability even after 60 days. This indicates that the THS-coated Fe_3O_4 magnetic fluid does not have any phase separation for a long time and uniformly dispersed in liquid carrier since THS coated evenly on the

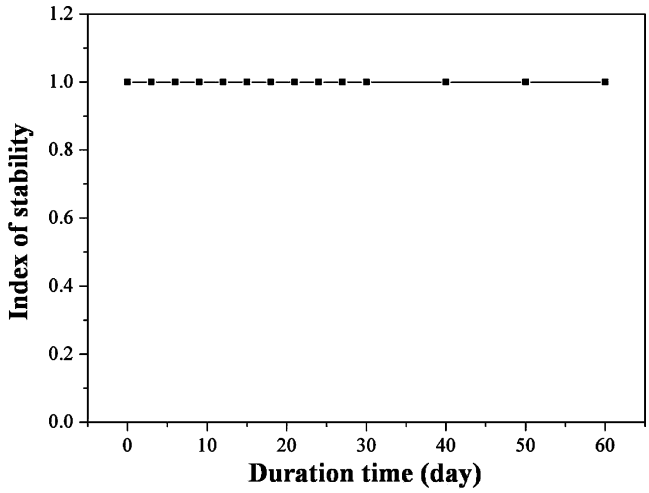

Figure 13. Stability index of magnetic fluid consisting of THS-coated Fe_3O_4 nanoparticles for desorption and degradation of coated THS versus the duration time.

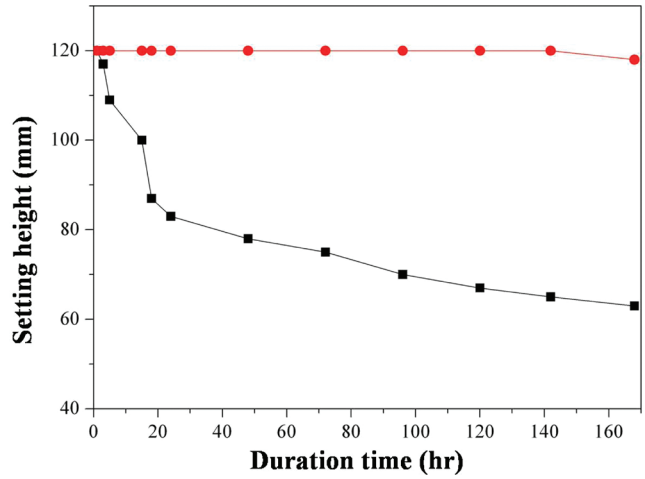

Figure 14. Dispersion stability of magnetic fluid consisting of oleic acid (■)- and THS (●)-coated Fe_3O_4 nanoparticles under acidic condition of pH 4 versus the duration time.

surface by covalent bonding of the OH group of magnetic nanoparticles. The duration lasted longer than 60 days. Figure 14 shows that the experimental results for the comparative dispersion stabilities of the conventional magnetic fluid consisting of oleic acid-coated Fe_3O_4 magnetic fluid and THS-coated Fe_3O_4 magnetic fluid under acidic condition of pH 4 versus duration time. In the case of the conventional magnetic fluid consisting of oleic acid-coated Fe_3O_4 magnetic fluid, the Fe_3O_4 magnetic particles have been sedimented extremely in an hour. It is thought that oleate coated on the surface of the Fe_3O_4 magnetic particle surface by weakly electrostatic interaction is dissociated from the surface of Fe_3O_4 magnetic particles due to attacking free acids in the liquid carrier. On the other hand, the magnetic fluid consisting of THS-coated Fe_3O_4 magnetic particles does not show any sedimentation in the magnetic fluid even after 60 days. From the results, we confirm that the stability of dispersion of the magnetic fluid consisting of THS-coated Fe_3O_4 magnetic nanoparticles is superior to that of the conventional magnetic fluid consisting of oleate-coated Fe_3O_4 magnetic nanoparticles.

Conclusions

In this study, we have explored the preparation method of a new magnetic fluid that comprises a colloidal dispersion of Fe_3O_4 magnetic particles covered with a monomolecular adsorbed film composed of THS and nonpolar hydrocarbon oil as liquid carrier. Fe_3O_4 magnetic particles were synthesized at pH 11.5 by precipitation of an iron salt solution in the basic solution after adjusting the mole ratio of Fe^{2+}/Fe^{3+} to 0.5. The particle size distribution of synthesized Fe_3O_4 magnetic particles was determined as 7.5 nm in the TEM image. The stability of the magnetic fluid consisting of Fe_3O_4 magnetic particles surface coated with THS was proved by no phase separation even after 60 days.

Acknowledgment. This work was supported by the Nano R&D Program of National Research Foundation and Brain Korea 21.

References and Notes

(1) Papel, S. S. U.S. Patent No 3215572, 1965.
(2) Rosensweig, R. E. *Encycl. Dictionary Phys., Suppl.* **1971**, *4*, 111.
(3) Cha, H. G.; Kim, Y. H.; Kim, C. W.; Lee, D. K.; Moon, S. D.; Kwon, H. W.; Kang, Y. S. *J. Nanosci. Nanotechnol.* **2006**, *6*, 3412.
(4) Han, Y. C.; Cha, H. G.; Kim, C. W.; Kim, Y. H.; Kang, Y. S. *J. Phys. Chem. C* **2007**, *111*, 6275.
(5) Cha, H. G.; Lee, D. K.; Kim, Y. H.; Kim, C. W.; Lee, C. S.; Kang, Y. S. *Inorg. Chem.* **2008**, *47*, 121.
(6) Hafeli, U. *Scientific and Clinical Applications of Magnetic Carrier*; Plenum Press, New York, 1999.
(7) (a) Shimoiizaka, J.; Nakatsuka, K.; Chubachi, R.; Sato, Y. *J. Chem. Soc. Jpn.* **1976**, *1*, 6. (b) Reimer, P.; Jahnke, N.; Schima, M.; Deckers, F.; Marx, F.; Holzknecht, N.; Saini, S. *Radiology* **2000**, *217*, 152.
(8) Sambucetti, C. J. *IEEE Trans. Magn.* **1980**, *16*, 382.
(9) Bacri, J. C.; Cabuil, V.; Massart, R. *J. Magn. Magn. Mater.* **1990**, *85*, 27.
(10) Reimer, G. W.; Khalafalla, S. E. U.S. Patent No. 4208294, 1980.
(11) Sato, T. *IEEE Trans. Magn.* **1970**, *6*, 795.
(12) Cullity, B. D. *Elements of X-ray Diffraction*, 2nd ed.; Addison-Wesley Pub. Co.: Reading, MA, 1978; pp 101−102.
(13) Berkowitz, A. E. *IEEE Trans. Magn.* **1980**, *16*, 184.
(14) Dunlop, D. J. *J. Geophys. Res.* **1978**, *78*, 1780.
(15) Whitehead W. E. U.S. Patent No. 4695393, 1987.
(16) Reimers, G. W. Khalafalla, S. E. *Bureau of Mines Innovative Process in Extraction Metallurgy Program*; Technical Process Report, 1972; p 59−74.
(17) Pileni, M. P. *Adv. Funct. Mater.* **2001**, *11*, 323.
(18) Moumen, N.; Pilei, M. P. *Chem. Mater.* **1996**, *8*, 1128.
(19) Bonini, M.; Wiedenmann, A.; Baglioni, P. *J. Phys. Chem. B* **2004**, *108*, 14901.
(20) Moumen, N.; Pileni, M. P. *J. Phys. Chem.* **1996**, *100*, 1867.

JP912166B